Advances in Environmental Technology 2 (2021) 69-78

Iranian Reasearch Organization for Science and Technology (IROST)

Advances in Environmental Technology

Journal home page: https://aet.irost.ir/

Preparation and activity evaluation of n-p CuO/CeO_2ZrO_2 heterojunction photocatalyst for degradation of organic azo dye in wastewater under visible light irradiation

Aiman. M.A. Noman[1], Mohammed A. Alghobar[2], Sidduraiah Suresha[1*]

[1] *Department of Environmental Science, Yuvaraja's College,University of Mysore, Mysore, Karnataka, India.*

[2] *Department of Agricultural Research and Extension Authority, Ministry of Agriculture, Yemen.*

ARTICLE INFO

Article history:
Received 27 March 2021
Received in revised form
13 September 2021
Accepted 14 September 2021

Keywords:
p-n CuO/CeO_2-ZrO_2
Wastewater
Photocatalytic activity
Zo dye

ABSTRACT

In this paper, n-p CuO/CeO_2ZrO_2 heterojunction photocatalysts with different concentrations of p-CuO were prepared by an auto solution combustion method. The structural and optical properties of the photocatalyst were characterized by X-ray powder diffraction (XRD), X-ray spectrum (EDS), scanning electron microscopy (SEM), X-ray photoelectron spectroscopy (XPS), Brunauer-Emmett-Teller (BET) and UV–vis diffuse reflectance spectroscopy (DRS). The photocatalytic activity of the photocatalyst was evaluated by the degradation of an aqueous azo dye acid orange 7 (AO7) solution. Experiments were carried out to asset the effect of n-CuO loaded on the n-CeO_2ZrO_2 photocatalytic properties and determine the adsorption potential of azo dye on p-CuO/n-CeO_2ZrO_2 at different pH values. Potential degradation pathway for photocatalytic degradations has been proposed using some radical scavengers to evaluate intermediates. Under similar visible light conditions, the photodegradation rate of dye catalyzed by p-n CuO/ CeO_2ZrO_2 was much faster than that of n-type CeO_2ZrO_2. The sample with a p-n CuO/CeO_2ZrO_2 ratio of 0.021 presented the best photocatalytic activity, which was 35% higher than that of n-CeO_2ZrO_2.

1. Introduction

Wastewaters containing dyes generated from textile industries are regarded as a major source of environmental pollution, owing to the large volumes, complex composition and resistance to biodegradation of the effluents [1]. The majority of synthetic dyes currently used in the industry are azo dyes and their derivatives because they are highly stable during washing, lightfast and not susceptible to degradation under natural conditions [2]. Azo dyes cause public health problems due to benzidine and aromatic rings which are contained within their structures, known carcinogens [3]. Among monoazo dyes acid orange 7 is the most commonly used anionic dye because it is water soluble, inexpensive and dyes rather quickly in weak acidic solution. Because of these properties, it is extensively used for dying a variety

*Corresponding author. Tel: 96063344635
E-mail: sureshakumar12@yahoo.com
DOI: 10.22104/AET.2021.4740.1283

of materials such as nylon, aluminum, detergents, cosmetics, wool and silk [4,5]. AO7 is highly toxic, and its ingestion can cause eye, skin, mucous membrane, and upper respiratory tract irritations; severe headaches; dizziness; nausea; and loss of bone marrow leading to anemia. Its consumption can also prove fatal, as it is carcinogenic in nature and can lead to tumors [6-8]. As a result, textile dyes in wastewaters must be treated and decolored using efficient and effective methods before being discharged into the environment. Heterogeneous photocatalysis assisted by various semiconductors has been considered as a cost-effective alternative as a pre- or post-treatment of biological treatment processes for the purification of dye-containing wastewater [9-11]. Among various metal oxide semiconductors, ZrO_2 (n-type) are widely used in a variety of technological fields owing to its unique photocatyalytic efficiency, nontoxidcity, low cost and high stability [12]. One obstacle to its effective utilization is the inefficient use of solar energy; less than 5% (UV light) of the sunlight can be absorbed by this photocatalyst. A simple and interesting approach to extend the catalyst absorption toward visible region is coupled semiconductors [13]. Cerium dioxide (CeO_2) catalysts have attracted much attention due to their high efficiency in visible light utilization. It is an n-type semiconductor with a relatively narrow band gap energy of 2.7 and 3.4 ev depending on the preparation technique [14]. It is extensively used as a technically important material in the application of water gas shift, solid oxide fuel cells, catalysis, oxygen sensors, glass polishing materials, ultraviolet absorbents, and photocatalyst for degradation of organic contaminants [15-17]. But the broad band gap energy and the electronic potential position in the conductance and valence bands of this material seriously limit its further application as a photocatalyst utilizing solar energy. A combination of two semiconductors with different gap level energies of type n-n junction (n-n CeO_2ZrO_2) exhibited better photocatalytic properties than single ones (n-ZrO_2). However, many strategies are commonly used to extend the spectral photoresponse of semiconductors such as doping with transition metals, dye sensitization and anionic doping. Besides, another promising idea is to couple them with narrow band gap semiconductors [18]. Because of its narrow band gap energy of 1.2-1.5 ev, as well as its catalytic, optical, electrical, and thermal properties, CuO (p-type) was chosen as a sensitizer semiconductor, it also has physical properties including superconductivity at high temperatures [19-21]. When CuO of p-type loading on the CeO_2ZrO_2 of n-type can form p–n junction photocatalyst; the inner electric field will also be produced in the interface. Once optical excitation occurs, a free electron (e^-) and an electronic vacancy (h^+) are formed, separated, and migrated effectively in a semiconductor being partially localized to the structural defective centers of its crystalline lattice ; hence improving the electrical properties of the semiconductor system [22]. In this work, the effect of p-CuO loading on the n-CeO_2ZrO_2 photocatalytic properties prepared by the process of solution combustion was studied. n-p CuO/CeO_2ZrO_2 was analyzed by (XRD), X-ray spectrum (EDS), scanning electron microscopy (SEM), X-ray photoelectron spectroscopy (XPS), Brunauer-Emmett-Teller (BET), and UV–Vis diffuse reflection spectrum (DRS). The effects of operational pH and amount of catalyst were investigated on the decolorization of azo dye. The n-p CuO/CeO_2ZrO_2 showed high photoactivity towards the degradation of azo dye and to be a promising alternative for dye containing wastewater treatment under visible light irradiation. The possible mechanisms of p–n junction formation and separation in photoexcited electron and hole were also investigated.

2. Materials and methods

2.1. Materials

Copper (II) Nitrate Trihydrate ($Cu(NO_3)_2.3H_2O$), Cerium (III) nitrate hexahydrate ($Ce(NO_3)_3.6H_2O$), Zirconyl nitrate ($ZrO(NO_3)_2$), ammonia, glycine, hydrochloric acid and sodium hydroxide. All of the chemicals were used without being purified further. Throughout the research, deionized water was used.

2.2. Photocatalysts preparation

The auto solution combustion process was used to synthesize p-n CuO/CeO_2ZrO_2 heterojunction photocatalysts using glycine as fuel at 400 °C. In

the percentage synthesis of 0.00, 0.02, 0.04, 0.06 and 0.08 M respectively of copper (II) nitrate trihydrate Cu $(NO_3)_2.3H_2O$, 0.3 M of cerium (III) nitrate hexahydrate $Ce(NO_3)_3.6H_2O$ and 0.3 M of zirconyl nitrate $ZrO(NO_3)_2.H_2O$, the stoichiometric composition of the solution mixtures (oxidizer and fuel) was measured in 10 ml of distilled water for each of each solution. The solutions were carefully combined by stirring well at room temperature for 1 hour to create an adsorption balance. Then, 0.1 M glycine (NH_2CH_2COOH) was separately dissolved in 20 ml of distilled water and added drop by drop under continuous stirring at 80 °C to the mixture. In order to adjust the pH to 7, a small amount of ammonia was used. The viscous blue colour of the gel was produced after 40 minutes. The gel temperature was increased to 200 °C and the process of auto ignition began and the final product was collected as an ash precipitate. The product was thoroughly washed for 5 minutes with ethanol, followed several times by distilled water, and centrifuged at 6,000 rpm. The collected product was dried for 120 minutes in a vacuum desiccator oven at 60 °C. Finally, the sample was ground into a pestle mortar and heated for 4 h in a muffle furnace in a crucible at 400 °C [23,24].

2.3. Photocatalyst characterization techniques

The powder crystal structures were characterized by X-ray diffraction (XRD, Proto, Canada) experiments of Cu Ka radiation were at room temperature. The X-ray spectrum (EDS) energy dispersive technique using (JSM-IT300, JEOL, Japan) were used to characterize the elemental composition. The morphology of the photocatalyst was inspected operating at 10 kV using SEM German LEO-1530 VP electron microscope. The catalyst's surface area of the Brunauer-Emmett-Teller (BET) was estimated to determine nitrogen adsorption at 77K (Quantachrome Autosorb-1model). X-ray photoelectron spectroscopy (XPS) was conducted on the Axis Ultra DLD. V. UV-vis absorption spectra were recorded on the SHIMADZU UV-3600 spectrometer.

2.4. Evaluation of photocatalytic activity

In order to assess the photocatalytic activity of degradation azo by p-n heterojunction photocatalysts CuO/ CeO_2-ZrO_2 under visible light radiation. The photocatalyst was separately distributed into an aqueous solution (100 ml) of azo dye (25 mg/L) at different concentrations. For 30 minutes in darkness, the suspension was well stirred to reach the adsorption equilibrium. The mixture was magnetically stirred under visible light irradiation. At regular intervals, the samples of 10 ml were collected from the suspension and centrifuged at 5000 rpm for 10 min. The concentration of aqueous azo dye was determined by using a UV-vis spectrophotometer (Shanghai UV-722). It showed the photocatalytic degradation rated ($C_t/C_{0)}$ of the dye on the p-n junction CuO/CeO_2 ZrO_2 and n-CeO_2 ZrO_2 photocatalysts, where C_t and C_0 referred to the equilibrated and the original dye concentrations.

3. Results and discussion

3.1. Photocatalytic materials characterization

X-ray diffraction (XRD) was investigated the crustal structure of p-CuO/n-CeO_2-ZrO_2 heterojunction photocatalysts prepared with various Cu $(NO_3)_2.3H_2O$ concentrations. All the diffraction peaks for CeO_2ZrO_2 on the 2θ scale at 28.6°(111), 33.2°(200), 47.5°(220), 56.4°(311), and 59.2°(203) planes shown in Figure 1 tetragonal, monoclinic phase of ZrO_2 along with the CeO_2 fluorite phase is clearly exhibited. Additional phases such as Cu, CuO, Cu_2O cannot be found in all samples that were too tiny to be detected by XRD (less than 3 nm) or well scattered on the n-CeO_2ZrO_2 photocatalyst assigned to Cupric oxide particles [25,26]. Also, the observed that the intensity of photocatalyst diffraction peaks increased with the amount of insertion of Cu $(NO_3)_2.3H_2O$. According to the JCPDS results, all diffraction peaks can be identified and assigned (#43-1002 for CeO_2 and #81-1544 for t-ZrO_2 and 81-1314 for m-ZrO_2). The crystallography was examined by determining the average crystal size of the synthesized nanoparticles using Derby Scherer's equation. The sample's crystal size was estimated through the full width of the half maximum intensity (FWHM) of mean reflectance (111) peak of the XRD patterns.

$$D = \frac{0.9\lambda}{\beta\cos\theta} \quad (1)$$

where D represents the crystalline size (nm), β signifies the diffraction line's entire width at half of the maximum intensity that is computed in

radians, λ denotes the X-ray wavelength of Cu Kα= 0.154 nm and θ represents the Bragg angle. Table 1 demonstrates the crystal size in the 6.9-8.3 nm range.

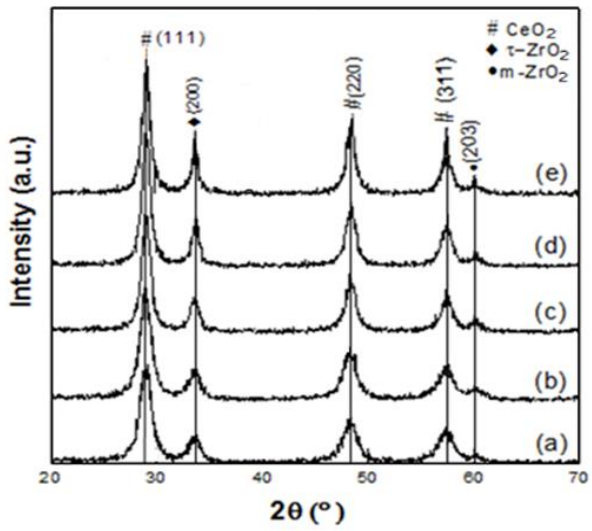

Fig. 1 XRD patterns of the CuO/CeO_2ZrO_2 heterojunction photocatalysts prepared with different concentrations of Cu $(NO_3)_2.3H_2O$ solutions: (a) n-CeO_2ZrO_2 (b) 0.02 M, (c) 0.04 M, (d) 0.06 M and (e) 0.08 M.

EDX technique was used to check the existence and importance of CuO in the Cu/CeO_2ZrO_2 nanoparticles since CuO cannot be detacted by XRD. The spectra and atomic composition of CuO/CeO_2ZrO_2 nanoparticles were presented in Figure 1 and Table.1. Equivalent peaks of elements (Cu, Ce, Zr and O) generated in the sputtered sample affirmed the present of CuO/CeO_2ZrO_2 nanoparticles. The ratio of CuO to CeO_2ZrO_2 in composites (0.02, 0.04, 0.06 and 0.08 M) were determined to be 0.014, 0.018, 0.021 and 0.025, which increase with Cu $(NO_3)_2.3H_2O$ concentrations. The outcome also shows that the CuO content dispersed on CeO_2ZrO_2 particles is so small that it is impossible to strongly crystalline. The morphology of CuO/CeO_2ZrO_2 catalyst prepared with 0.06 M Cu $(NO_3)_2.3H_2O$ was investigated by SEM micrographs. Figure 3b. shows the image of small particles with a uniform distribution is adhere to the CeO_2ZrO_2 nanoparticles. The small particles are considered to be CuO. The particles sizes were in the range of 8–15 nm and in good accord with X-ray diffraction analysis. XPS was used to verify p-CuO on the surface of the n-CeO_2ZrO_2 particles. The Cu 2p, Ce 3d, O 1s, C 1s, and Zr 3d peaks validate the presence of Cu, Ce, O, C, and Zr from the survey spectrum (Figure 3a). The presence of the tiny C 1s peak comes from atmospheric pollution and adsorbed impurities. In the binding energies of 952.9 and 932.9 eV, respectively, the peaks of Cu $2p_{1/2}$ and Cu $2p_{3/2}$ appear from (Figure 3b), which also suggests the presence of CuO, because Cu $2p_{1/2}$ and Cu $2p_{3/2}$ shake up intensively at binding energies of 961.9 and 942.0 eV, respectively, which are the characteristic peaks of CuO [27,28].

Table.1. Elemental composition, textural properties and size of heterojunction photocatalysts p-CuO/n-CeO_2ZrO_2

S[a]	Ce (wt%)	Zr (wt%)	Cu (wt%)	O (wt%)	C (wt%)	CuO/CeO_2ZrO_2	BET surface area(m^2/g)	Pore diameter (Å)	Pore volume (cm^3/g)	Crystallite size (nm)
1	-	-	-	-	-	-	70	257	0.51	7.2
2	31.53	14.45	2.11	29.70	22.21	0.014	66	96	0.56	7.09
3	30.08	14.98	3.05	29.50	23.39	0.018	65	116	0.29	6.39
4	30.88	14.20	3.46	29.31	23.15	0.021	64	139	0.18	8.6
5	32.93	12.81	4.27	29.54	20.45	0.025	58	189	0.17	7.6

Samples are prepared with different concentrations of (Cu $(NO_3)_2.3H_2O$): (1) 0,00(2) 0.02, (3) 0.04, (4)0.06 and (5) 0.08 M.

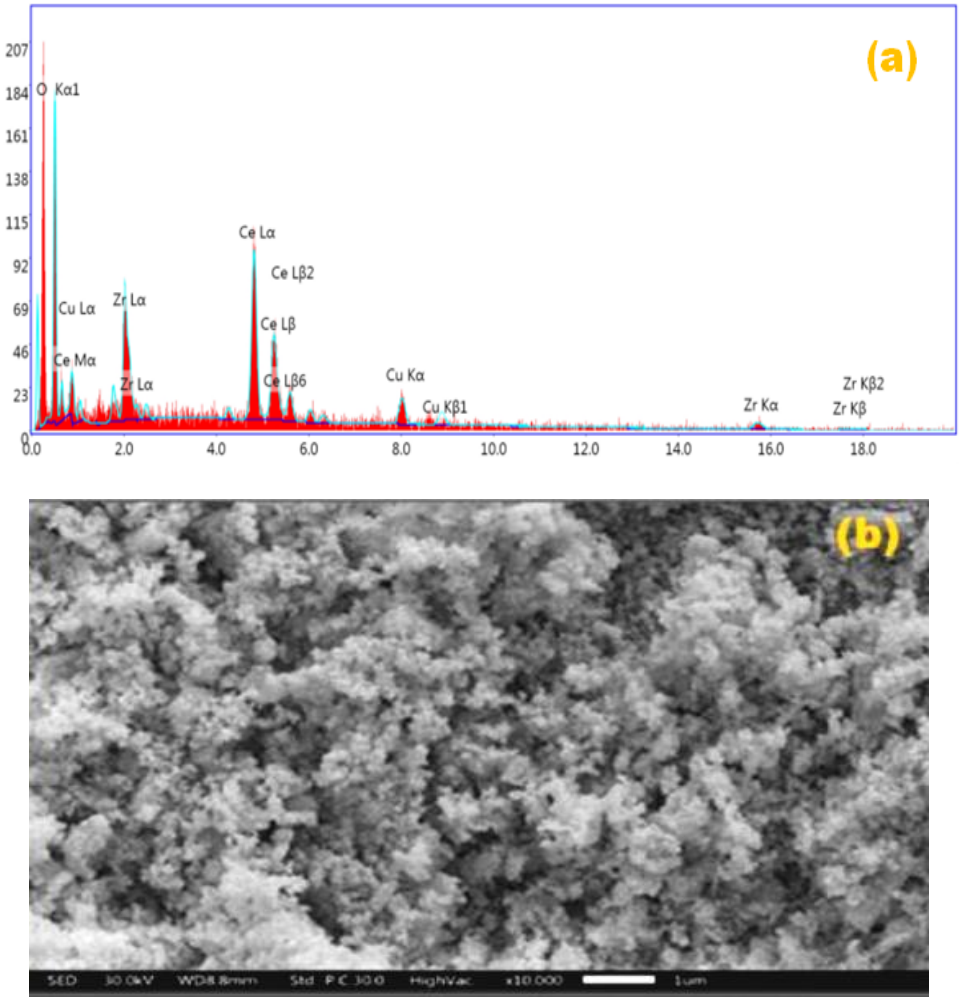

Fig.2 (a) EDS analysis and (b) SEM image of p-n CuO/CeO_2ZrO_2 heterojunction photocatalyst prepared with 0.06 M $Cu(NO_3)_2.3H_2O$.

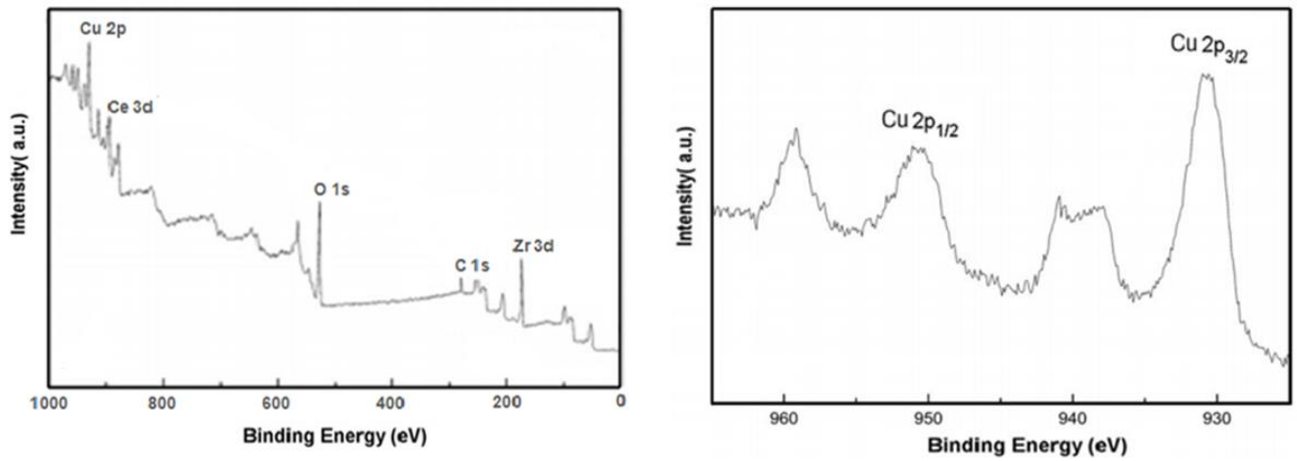

Fig.3. The survey (A) and Cu 2p3/2 (B) XPS spectra of the n-CuO/p-CeO_2ZrO_2 composite prepared with 0.06 M $Cu(NO_3)_2.3H_2O$.

3.1.1. Textural properties

The nitrogen adsorption-desorption isotherms are the same in all synthesised oxides (n-CeO_2ZrO_2 and p-CuO/n-CeO_2ZrO_2). Figure 4 and Table 1 show the nitrogen isotherm and textural properties of photocatalysts, respectively. The only difference in the isotherms of these photocatalysts is in the absorbed volumes, which show different specific surface area results. The BET specific surface area the p-CuO/n-CeO_2ZrO_2 photocatalysts decreased with the increase of p-CuO loading, revealing a difference in the specific surface areas.

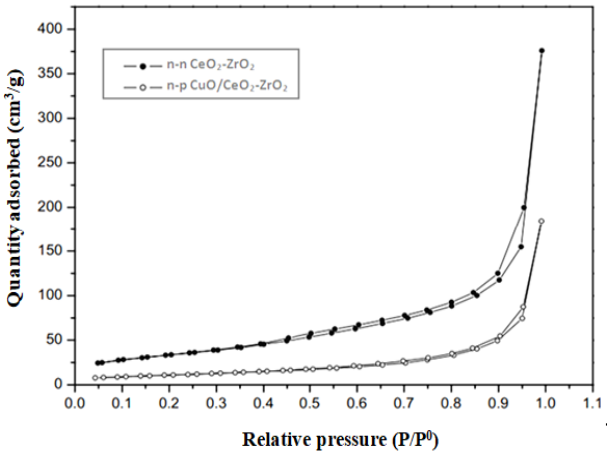

Fig.4. N_2 adsorption-desorption isotherms of n-CeO_2ZrO_2 and n-p CuO/CeO_2ZrO_2photocatalysts.

3.2. Photocatalytic Activity

The photocatalytic activity of mixture nanoparticles was investigated in the photodegradation of azo dye under visible light (> 420 nm) irradiation. The amount of p-CuO in a mixture of n-CeO_2-ZrO_2 has an effect on the photocatalytic activity of azo dye degradations, as shown in Figure 5. As seen, the highest reactivity is obtained for the mixture of n-CeO_2ZrO_2 with X_{CuO} = 0.06. The degradation efficiencies in duration 90 min obtained 70.05, 75.35, 84.50 and 80.75% for the amount of X_{CuO}= 0.02, 0.04, 0.06 and 0.08 respectively. While only 64.80% of AO7 can be decomposed using n-type CeO_2-ZrO_2 as photocatalyst. That is to say, the results indicate that the amount of p-CuO loading on the n-p CuO/CeO_2-ZrO_2 can play an important role in the photocatalytic performance because a small amount of p-CuO can't effectively separate electrons and holes photogenerated from the photocatalyst, resulting in low photocatalytic activity. On the other hand, as shown in the sample prepared with 0.08 M $Cu(NO_3)_2.3H_2O$, an excess of CuO will reduce the photocatalytic activity of the photocatalyst.

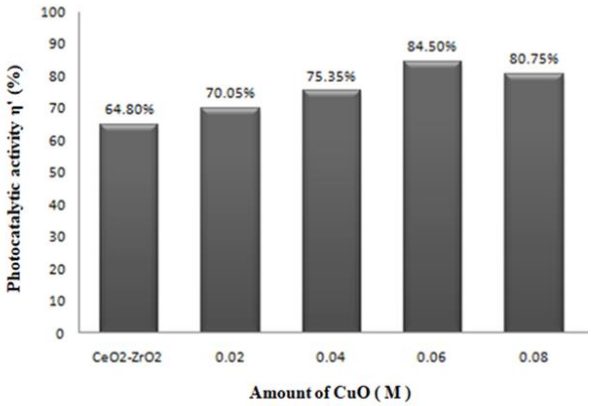

Fig.5 The Effect of the amount of CuO on the photocatalytic activity of n-p CuO/CeO_2ZrO_2 For photodegradation of AO7 under visible light irradiation ([Catalyst] = 0.1 g/L, [AO 7]= 75 mg/L, pH= 7.

Figure 6 shows the UV-vis diffuse reflectance spectra (DRS) of n-type CeO_2ZrO_2 and p-type CuO loaded n- CeO_2ZrO_2 (prepared in 0.06 M $Cu(NO_3)_2.3H_2O$ solution). It demonstrates that the p-n CuO/CeO_2ZrO_2 heterojunction photocatalysts have a visible red shift and increased absorption. The optical band gap energy (Eg) of the powders was determined using the equation Eg=1240/ Absorp.Edge. n-CeO_2ZrO_2 and p-n CuO/CeO_2ZrO_2 indicate band gap absorption onset at 460 and 472 nm, respectively, corresponding to band gap energies of 2.70 and 2.62 eV. As a result, when compared to n-CeO_2ZrO_2, the optical absorption edge of the p-n CuO/CeO_2ZrO_2 composite moves to a lower energy region, and its absorption is stronger in the wavelength range of 400–600 nm. That is, the p-n CuO/CeO_2ZrO_2 composite photocatalyst has a higher optical absorption capacity than n-type CeO_2-ZrO_2 and can produce more photo-introduced electrons/hole pairs under visible light.

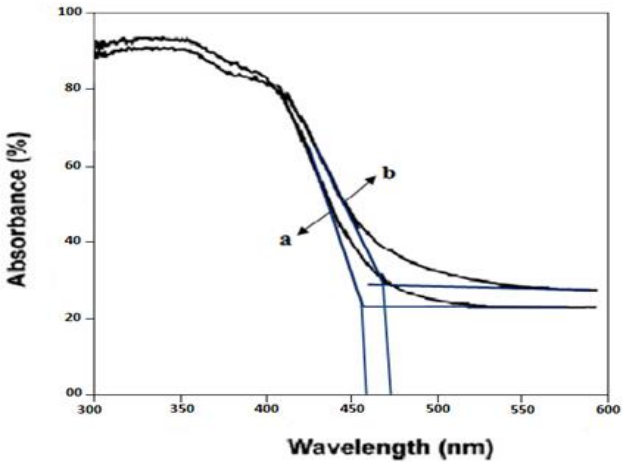

Fig.6 UV-vis diffuse reflectance spectra of (a) n-CeO_2ZrO_2 and (b) p-n CuO/CeO_2ZrO_2 heterojunction prepared with 0.06 M Cu $(NO_3)_2.3H_2O$.

3.3. pH effect on adsorption

The adsorption potential of dyes on photocatalysts is well known to be a key factor in the rate of degradation in photocatalytic systems. Therefore, to explain the enhanced photocatalytic activity of p-n CuO/CeO_2ZrO_2 as compared to the n-CeO_2ZrO_2, the adsorption of azo dye on p-n CuO/CeO_2ZrO_2 and n-CeO_2ZrO_2 nanoparticles were examined. The pH of the samples was controlled using hydrochloric acid and sodium hydroxide (0.01 M) and a Metrohm pH-meter with combined electrode. The adsorption capacity of samples prior to (A_o) and after (A_t) irradiation, as well as Beers' law for determining C_o and C_t, are used to calculate degradation efficiency (Eq. (1)).

$$\%\text{Degradation} = 100\times [1-\frac{Ct}{Co}] = 100 \times [1-\frac{At}{Ao}] \quad (1)$$

Figure.7 shows the photodegradation of AO7 (75 mg/L) by a photocatalyst (0.1 g/L) over a 120-minute duration at various pH. Azo dye has the fastest degradation rate at pH 3. The rates of azo dye degradation were pH-dependent where getting down as the pH values rise. An increase in pH can lead to a decrease in adsorption and consequently a decrease in degradation rate. Therefore, we can conclude that adsorption capacity played a key role in determining photocatalytic degradation efficiency of azo dyes over n-p CuO/CeO_2ZrO_2.

3.4. Mechanism of degradation

The p-CuO/n-CeO_2ZrO_2 photocatalysis mechanism (based on the CB & VB) is graphically presented in scheme.1. The enhanced photogenerated charge separation of the p-CuO/n-CeO_2ZrO_2 can be attributed to an improvement in photocatalytic activity of catalyst. The band gap of p-Cu/n-CeO_2ZrO_2 was 2.62 eV, which was excitable by visible light. Improved optical absorption is probably one of the factors contributing to the increased activity of the p-Cu/n-CeO_2ZrO_2 composite [29,30]. CeO_2ZrO_2 of n-type and CuO of p-type semiconductors can form p–n junction photocatalysts when CuO is loaded on the n-CeO_2ZrO_2 surface, which is favorable for the separation of photogenerated charges. Thus, The holes flow into the negative field, while the electrons flow into the positive field, due to the influence of the inner electric field. As a result, the photogenerated electron-hole pairs were separated more effectively. A large increase in the life-time of the photogenerated electron-hole pair was observed due to electron and hole transfer in the p-n CuO/CeO_2ZrO_2 heterojunction. These electron/hole pairs are free to start a chain reaction that will eventually mineralize the azo dye. $O_2^{\bullet-}$ and $OH^{\bullet}$, as highly oxidative radical species, were generated with the electrons captured by the adsorbed oxygen molecules and h^+ trapped by the surface hydroxyl, respectively. Generally, under visible light irradiation, the degradation of azo dye by p-n CuO/CeO_2ZrO_2 in aqueous solution is caused by the production of reactive oxygen species ($O_2^{\bullet}$ and $OH^{\bullet}$) and holes (h^+).

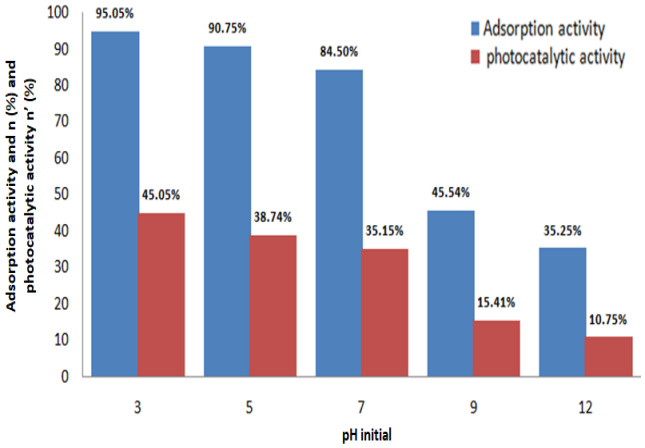

Fig.7 Effect of the pH solution on the photocatalytic redox of AO7 under visible light irradiation CuO/CeO_2ZrO_2= 0.1 g/L, AO7 = 75 mg/L, irradiation time = 120 min.

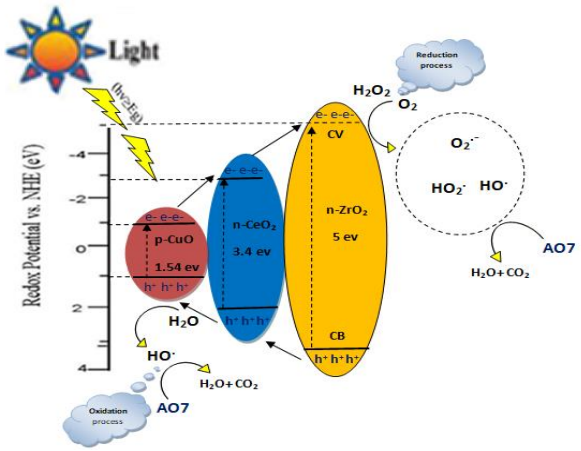

Scheme.1. The photocatalytic mechanism over n-p CuO/CeO_2ZrO_2 heterojunction photocatalyst under irradiation of visible light.

3.5. Active species to attack dye molecule

In order to determine the main active species responsible for the degradation of dye molecules, the scavenger's isopropanol (IPA), benzoquinone (BQ) and disodium ethylenediamine tetra-acetate (EDTA) were used to trap hydroxyl radical ($OH^{\bullet}$), superoxide radicals ($O_2^{\bullet-}$) and positive holes (h^+), respectively. Figure 8 displays the relationship of different scavengers and the photodegradation of azo dye solution in the presence of S4 photocatalyst. It was discovered that EDTA does not deactivate the photocatalyst in a significant way. While, the addition of IPA and BQ, on the other hand, completely inhibited the photocatalytic process. These findings clearly demonstrated that superoxide radicals ($O_2^{\bullet-}$) and hydroxyl radicals ($OH^{\bullet}$) were the most reactive oxygen species involved in the AO7 degradation process.

4. Conclusions

Under visible light irradiation (I>420 nm), the photocatalytic activity of p-CuO loading on n-CeO_2ZrO_2 to degrade azo dye was examined, it was found to have better efficiency than n-CeO_2ZrO_2. The photocatalyst prepared in 0.06 M $Cu(NO_3)_2.3H_2O$ solution has the best photocatalytic activity. The effect of initial solution pH on photocatalysts adsorption capacity was studied, the lower the pH, the more p-n CuO/CeO_2ZrO_2 is adsorbed, resulting in a faster degradation rate. Superoxide radicals ($O_2^{\bullet-}$) and hydroxyl radicals ($OH^{\bullet}$) were discovered to be responsible for attacking the dye molecules, and these radicals were detected indirectly by using various radical scavengers. The formation of the p–n junction and improved visible light absorption could explain the increased photocatalytic degradation.

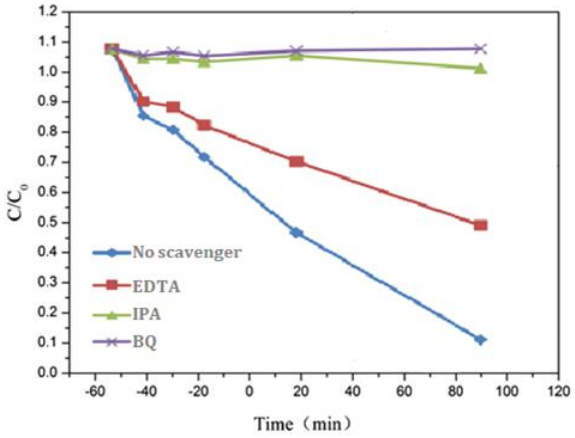

Fig.8 Effects of different scavengers on AO7 photodegradation using n-p CuO/CeO_2ZrO_2 heterojunction photocatalyst under visible light irradiation.

References

[1] Shiping, Xu., Jiawei, Ng., Xiwang, Z., Hongwei, B., Darren, S. (2011). Adsorption and photocatalytic degradation of Acid Orange 7 over hydrothermally synthesized mesoporous TiO_2 nanotube. *Colloids and surfaces A: physicochemical and engineering aspects*, *379* (1–3), 169-175.

[2] Sergi, G., Sergi, D.b., Josep, M., Guilemany, b., Enric, B. (2013). Solar photoelectrocatalytic degradation of Acid Orange 7 azo dye using a highly stable TiO_2 photoanode synthesized by atmospheric plasma spray. *Applied catalysis B: environmental*, *133*(27), 142-150.

[3] Nematollah, J., Sahand, J., Farshid, G., Mehdi, A., Gelavizh, B. (2018). The performance study on ultrasonic/Fe_3O_4/H_2O_2 for degradation of azo dye and real textile wastewater treatment. *Journal of molecular liquids*, *256*(15), 462-470.

[4] Esther, F., Tibor C., Gyula, O. (2004). Removal of synthetic dyes from wastewaters. *Environment international*, *30*(7), 953-971.

[5] Gupta, V. K., Mittal, A., Gajbe, V., Mittal, J. (2006). Removal and recovery of the hazardous azo dye acid orange 7 through adsorption over

waste materials: bottom ash and de-oiled soya. *Industrial and engineering chemistry research*, *45*(4), 1446-1453.

[6] Aber, S., Daneshvar, N., Soroureddin, S. M., Chabok, A., Asadpour-Zeynali, K. (2007). Study of acid orange 7 removal from aqueous solutions by powdered activated carbon and modeling of experimental results by artificial neural network. *Desalination*, *211*(1-3), 87-95.

[7] Özcan, A., Oturan, M. A., Oturan, N., Şahin, Y. (2009). Removal of Acid Orange 7 from water by electrochemically generated Fenton's reagent. *Journal of hazardous materials*, *163*(2-3), 1213-1220.

[8] Greluk, M., Hubicki, Z. (2011). Efficient removal of Acid Orange 7 dye from water using the strongly basic anion exchange resin Amberlite IRA-958. *Desalination*, *278*(1-3), 219-226.

[9] Ji, P., Zhang, J., Chen, F., Anpo, M. (2009). Study of adsorption and degradation of acid orange 7 on the surface of CeO_2 under visible light irradiation. *Applied catalysis B: environmental*, *85*(3-4), 148-154.

[10] Muhd Julkapli, N., Bagheri, S., Bee Abd Hamid, S. (2014). Recent advances in heterogeneous photocatalytic decolorization of synthetic dyes. *The scientific world journal*, *2014*.

[11] Antonopoulou, M., Kosma, C., Albanis, T., & Konstantinou, I. (2020). An overview of homogeneous and heterogeneous photocatalysis applications for the removal of pharmaceutical compounds from real or synthetic hospital wastewaters under lab or pilot scale. *Science of the total environment*,*765,* 144163.

[12] Zhao, J., Gea, S., Pana, D., Shao, Q., Linb, J., Wangc, Z., Hud, Z., Wue, T., Guo, Z. (2018). Solvothermal synthesis, characterization and photocatalytic property of zirconium dioxide doped titanium dioxide spinous hollow microsphereswith sunflower pollen as bio-templates. *Journal of colloid and interface science*, *529*,111-121.

[13] Pirzada, B. M., Mir, N. A., Qutub, N., Mehraj, O., Sabir, S., Muneer, M. (2015). Synthesis, characterization and optimization of photocatalytic activity of TiO_2/ZrO_2 nanocomposite heterostructures. *Materials Science and engineering: B*, *193,* 137-145.

[14] Kusmierek, E. (2020). A CeO_2 Semiconductor as a Photocatalytic and photoelectrocatalytic material for the remediation of pollutants in industrial wastewater: A review. *Catalysts*, *10*(12), 1-54.

[15] Bakkiyaraj, R., Bharath, G., Ramsait, K. H., Abdel-Wahab, A., Alsharaeh, E. H., Chen, S. M., Balakrishnan, M. (2016). Solution combustion synthesis and physico-chemical properties of ultrafine CeO_2 nanoparticles and their photocatalytic activity. *RSC advances*, *6*(56), 51238-51245.

[16] Prabhu, S., Viswanathan, T., Jothivenkatachalam, K., Jeganathan, K. (2014). Visible light photocatalytic activity of CeO_2-ZnO-TiO_2 composites for the degradation of rhodamine B. *Indian journal of materials science*, *2014, 1-10*.

[17] Ahmad, U.R., Kumar, M.S., Akhtar, G., Kumar, S.H., Kim. (2015). Growth and properties of well-crystalline cerium oxide (CeO_2) nanoflakes for environmental and sensor applications. *Journal of colloid and interface science*, *454*(15), 61-68.

[18] Hu, S., Zhou, F., Wang, L., Zhang, J., (2011). Preparation of Cu_2O/CeO_2 heterojunction photocatalyst for the degradation of Acid Orange 7 under visible light irradiation. *Catalysis communications*, *12*(9),794–797.

[19] SILVA, W. J. D., SILVA, M. R., Takashima, K. (2015). Preparation and characterization of Zno/CuO semiconductor and photocatalytic activity on the decolorization of direct red 80 azodye. *Journal of the chilean chemical society*, *60*(4), 2749-2751.

[20] Asl, I.M., Ghazi, M.M., Jahangiri M. (2016). Synthesis, characterization and degradation activity of Methyl orange Azo dye using synthesized CuO/α-Fe_2O_3 nanocomposite. *Advances in environmental technology,* 4, 169-177.

[21] Zoolfakar, A. S., Rani, R. A., Morfa, A. J., O'Mullane, A. P., Kalantar-Zadeh, K. (2014). Nanostructured copper oxide semiconductors: a perspective on materials, synthesis methods and applications. *journal of materials chemistry c*, *2*(27), 5247-5270.

[22] Liu W., Chen S., Zhang S., Zhao W., Zhang H., Yu X. (2010). Preparation and characterization

of p–n heterojunction photocatalyst p-$CuBi_2O_4$/n-TiO_2 with high photocatalytic activity under visible and UV light irradiation. *Journal of nanoparticle research*, *12*, 1355–1366.

[23] Wen, W., and Wu, J. (2014). Nanomaterials via solution combustion synthesis: a step nearer to controllability. *RSC advances*, *4*, 580–8100.

[24] Deganello, F., and Tyagi, A. (2018). Solution combustion synthesis, energy and environment: Best parameters for better materials. *Progress in crystal growth and characterization of materials*, *64*(2), 23-61.

[25] Hu, S., Zhou, F., Wang, L., Zhang, J., (2011). Preparation of Cu_2O/CeO_2 heterojunction photocatalyst for the degradation of Acid Orange 7 under visible light irradiation. *Catalysis communications*,*12*(9),794–797.

[26] Chan, Y. N., Hsu, R. S., Lin, J. J. (2010). Mechanism of silicate platelet self-organization during clay-initiated epoxy polymerization. *The journal of physical chemistry C*, *114*(23), 10373-10378.

[27] Mageshwari, K., Nataraj, D., Pal, T., Sathyamoorthy, R., Park, J. (2015). Improved photocatalytic activity of ZnO coupled CuO nanocomposites synthesized by reflux condensation method. *Journal of alloys and compounds*, *625*, 362-370.

[28] Yang, L., Chu, D., Wang, L. (2016). CuO core–shell nanostructures: precursor-mediated fabrication and visible-light induced photocatalytic degradation of organic pollutants. *Powder technology*, *287*, 346-354.

[29] Shifu, C., Sujuan, Z., Wei, L., Wei, Z. (2008). Preparation and activity evaluation of p–n junction photocatalyst NiO/TiO_2. *Journal of hazardous materials*, *155*(1-2), 320-326.

[30] Chen, S., Zhao, W., Liu, W., & Zhang, S. (2008). Preparation, characterization and activity evaluation of p–n junction photocatalyst p-ZnO/n-TiO_2. *Applied surface science*, *255*(5), 2478-2484.